Consequences of sawteeth on TAE activity in fusion plasmas

F. Jaulmes[1], S. D. Pinches[2], E. Westerhof[1] and JET EFDA contributors

[1]*FOM Institute DIFFER, Nieuwegein, The Netherlands*

[2]*ITER Organization, Route de Vinon-sur-Verdon, 13115 St. Paul-lez-Durance, France*

1. Introduction

Fusion reactions produce high energetic He (alphas) particles (at $\mathscr{E}_0 \simeq 3.5MeV$) that heat the plasma through collisions with electrons, then ions, to maintain the proper rate of fusion reactions. When they are thermalized at ion temperature, they contribute to dilute and cool the plasma as any other impurities. Our purpose here is to evaluate if it is possible to evacuate the thermal helium by using a controlled version [1] in the sawtooth instability without triggering TAE activity in a JET-like and an ITER-like magnetic geometry.

2. Dynamical modelling of the sawtooth collapse and corresponding motions of fast ions

Pre-collapse equilibrium and resonant surface

We have used tokamak equilibria as obtained from the equilibrium code FINESSE [2]. We have developed a numerical model of the sawtooth collapse based on the original full reconnection pattern suggested by Kadomtsev [3] with the dynamical evolution of the electromagnetic fields during the collapse as introduced by Kolesnichenko et al. in [4]. The fast ions are evolved as described in [5]. The mixing radius r_{mix} is the post-crash position of the separatrix where, after the collapse, a discontinuity in q is present. After about 100ms the discontinuity is smoothed by current diffusion over a few millimeters. this is simulated numerically according to: $\frac{\partial q}{\partial t} = \frac{\eta}{\mu_0}\frac{\partial^2 q}{\partial r^2}$. We thus study the stability of the pre-crash, the post-crash and the post-current-diffusion configurations.

A typical equilibrium burning plasma

The energy is transferred from the alphas to the plasma by collisions, first with electrons, then with ions. We evaluate the source of fast alphas from fusion as $S_\alpha \sim \langle\sigma v\rangle\, n_i^2/4$ (see [6]). The alpha-particle distribution is modeled by a localized slowing down distribution according to their energy. We use the distribution functions (see [7]):

$$f_{\alpha h0} = \frac{\tau_s}{2\pi} S_\alpha \left[\frac{n_i}{n_e} + \left(\frac{v}{v_c}\right)^3\right]^{-1} \quad ,\mathscr{E} \le \mathscr{E}_0 \quad \text{and} \quad f_{\alpha h} = f_{\alpha h0} \exp\left[\frac{-m_\alpha(\mathscr{E}-\mathscr{E}_0)}{T m_i}\right] \quad ,\mathscr{E} > \mathscr{E}_0 \tag{1}$$

where τ_s is the global slowing down time and v_c is the critical velocity, defined as the change of collisional regime for the alphas from electron-dominated ($v > v_c$) to ion-dominated ($v <$

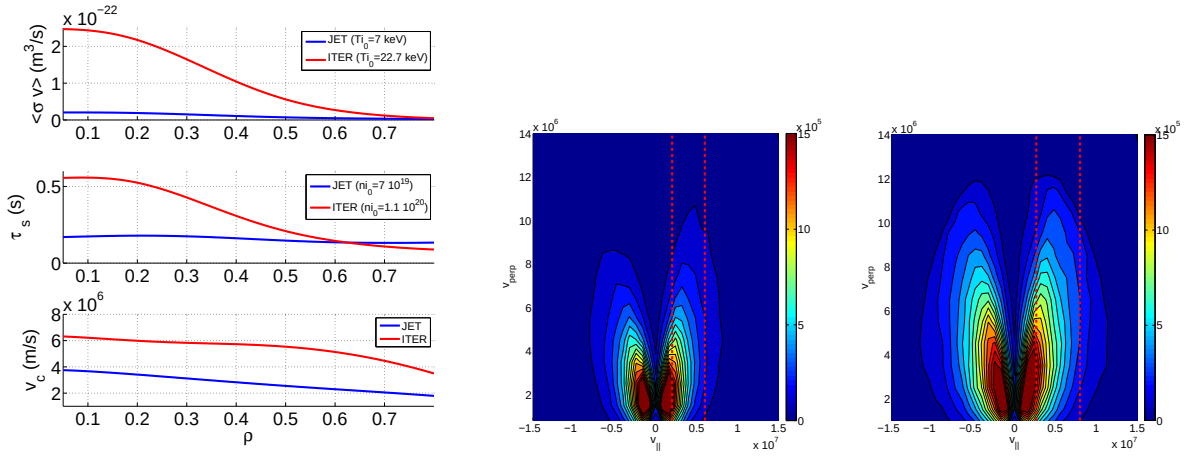

Figure 1: Left plot : parameters used to evaluate the initial distribution of alphas in a burning plasma (equation (1)) ; Right plots : compared passing alphas velocity space distribution around $q \simeq 1.1$ for JET (middle) and ITER (right).

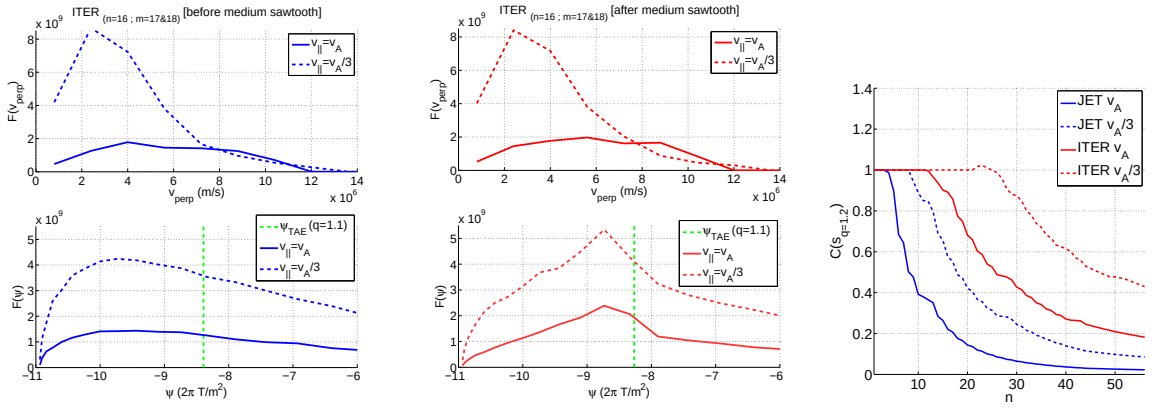

Figure 2: Left plots : distribution function at the different resonant velocities as a function of $v_\perp$ and ψ as they enter in the calculation of γ_α from the distribution of alphas ; Left: before crash and middle : after crash ; Right plot : compared effect of FOW coefficient for JET and ITER.

v_c). The resulting distribution in velocity space are shown on figure (1) for the JET and ITER configurations discussed in this paper.

3. Toroidal Alfvén eigenmodes in a burning DT plasma

Drive by energetic particles

The particles interact with the TAE at the resonant position where $q_{TAE} \simeq (m+1/2)/n$ and the drive they induce is derived according to [8]:

$$\frac{\gamma_\alpha}{\omega_{TAE}} = \frac{2\pi^2 \mu_0 m_{He}^2 R_0 q_{TAE}^3}{B_0^2} \left[\int_0^\infty \left(v_\parallel^2 + \frac{v_\perp^2}{2} \right) \left(\frac{\omega_{TAE}}{m_{He}} \frac{\partial F}{\partial v_\perp} - \left(\frac{n}{Ze} \frac{\partial F}{\partial \psi} \right) v_\perp \right) dv_\perp \Big|_{v_\parallel = v_A} + \ldots \Big|_{v_\parallel = v_A/3} \right] \quad (2)$$

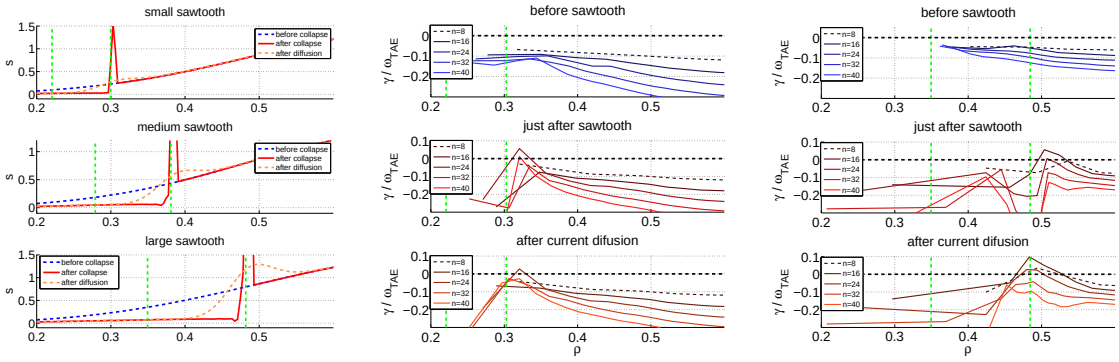

Figure 3: Left : evolution of the magnetic shear in ITER during increasingly larger sawteeth ; Right plots : compared destabilization in ITER for a small and large sawtooth.

where $\omega_{TAE} = v_A/(2q_{TAE}R_0)$. Since the population of alphas is highly peaked, we get strong radial gradients after the crash. Thus the term in $\partial F/\partial\psi$ is dominant for the evaluation of the drive. It turns out that the low alpha pressure in JET builds up a very small drive for the TAE. In this paper we thus only discuss results for ITER: the calculation for (2) is illustrated on figure (2). TAE stability study in JET is however relevant in NBI or ICRH heated plasmas.

Damping mechanisms

We consider the following mechanisms to be dominant for the damping of the high-n core TAEs discussed here: electron landau damping γ_e [8], Finite Orbit Width (FOW) effects [9] and radiative damping γ_{rad} [10]. The overall growth rate is expressed as: $\gamma = \frac{F(D)}{D}(\gamma_\alpha) + \gamma_{rad} + \gamma_e$.

γ_e is the electron Landau damping as given in [8] and remains small. FOW effects are necessary to explain the high-n limit of the TAEs. We use it as a multiplicative correction factor $F(D)/D$ to the drive given by (2) (where $D = \Delta_b/\Delta_{rTAE}$ is the ratio of the average orbit width of the alphas over an estimate of the radial width of the mode ; F is an integral given in [9]). The radiative damping is evaluated as:

$$\frac{\gamma_{rad}}{\omega_{TAE}} \simeq -\frac{3\sqrt{3}}{4}\left(\frac{nqs\rho_s}{r}\right)^{2/3} \quad ; \quad s = \frac{r}{q}\frac{\mathrm{d}q}{\mathrm{d}r} \quad ; \quad \rho_s = \frac{\sqrt{m_i T_e}}{eB} \tag{3}$$

5. TAE stability in an ITER-like configuration : effect of mixing radius position

Equilibria

The typical parameters considered are those of the planned ITER basic inductive scenario (scenario 2), where $P_0 \sim 8.9 \times 10^6$Pa is the pressure on the magnetic axis, $I_P \sim 15$MA is the global toroidal plasma current and $B_{axis} \sim 5.2$T is the total field on axis. The simulations were performed with the current in the same direction as that of the toroidal field. The Shafranov shift is ~ 0.05m for $\beta = (2\mu_0\langle P\rangle)/\langle B^2\rangle \sim 2.0\%$ (where $\langle P\rangle$ is the volume averaged pressure

of the plasma, B is the magnetic field).

Compared growth rate for different mixing radius position

We consider increasing sawtooth dimensions for the central safety factor values $q_0 = 0.96; q_0 = 0.94; q_0 = 0.88$. As the sawtooth size increases, so does the shear at the mixing radius. There is thus additional radiative damping for larger sawteeth. The mode structure in outer regions is also more narrow, allowing for additional FOW damping effects. Both effects contribute to balance (even maybe damp) the drive induced by large gradients of fast particles occurring with larger sawteeth.

As the current profile relaxes, the TAE radial structure changes, allowing a shift in the destabilized modes. As long as the fast particles gradient survives in the mixing region, a large panel of mode numbers may thus be excited.

6. Conclusion and outlooks

Whilst sawteeth that occur in high performance ITER plasmas may help expel Helium ash and impurities they may also destabilise TAE through changes to the fast ion distribution [5]. This work has used a simple model to estimate the change in the TAE drive due to the redistribution of alphas during a sawtooth. The damping is a subtle combination of radiative damping (high shear) and Finite Orbit Width (FOW) effects (mode radial extension).

Depending upon the consequences of unstable TAE, further work may be required to address their control and mitigation, for example through the use of the auxiliary heating systems. Further work will also try to refine the growth rate calculations by using a kinetic code to model the energy transfer between the energetic particles and the TAE. The goal will be to improve the modelling of FOW effects.

Acknowedgements
The work in this paper has been performed in the framework of the NWO-RFBR Centre of Excellence (grant 047.018.002) on Fusion Physics and Technology. This project has received funding from the European Union's Horizon 2020 research and innovation programme under grant agreement number 633053. The views and opinions expressed herein do not necessarily reflect those of the European Commission

References

[1] Chapman I. et al. 2011 *Plasma Phys. Control. Fusion* **53** 124003
[2] Keppens R. and Blokland J.W.S. 2006 *Fusion Sc. and Technol.* **49** 131
[3] Kadomtsev B. B. 1975 *Sov. J. Plasma Phys.* **1** 389
[4] Kolesnichenko Ya. I. and Yakovenko Yu. V. 1996 *Nucl. Fusion* **36** 159
[5] Jaulmes F. et al. 2014 *Nucl. Fusion* **SE** 2014 (submitted)
[6] Freidberg J. 2007 *Plasma Physics and Fusion Energy*, Cambridge University Press
[7] Hazeltime R. D. and Meiss J. D. 2003 *Plasma Confinement*, Dover Publications
[8] R. Betti and J. P. Freidberg 1992,*Phys. Fluids B* **6** 1465
[9] Breizman B. N. and Sharapov S. E. 1995 *Plasma Phys. Control. Fusion* **37** 1057
[10] Mett R. R., Strait E. J., Mahajan S. M. 1993,*Phys. Plasmas* **1** 3277